Nanoscale

RSC Publishing

PAPER

View Article Online
View Journal | View Issue

Cite this: *Nanoscale*, 2013, **5**, 5833

Label-free electrochemical impedance genosensor based on 1-aminopyrene/graphene hybrids

Li-qiang Luo,*[a] Zhao Zhang,[a] Ya-ping Ding,[a] Dong-mei Deng,[a] Xiao-li Zhu[b] and Zhen-xin Wang*[c]

Received 11th March 2013
Accepted 15th April 2013

DOI: 10.1039/c3nr01237a

www.rsc.org/nanoscale

In this work, we proposed a novel simple protocol for preparing 1-aminopyrene/graphene (ApG) hybrids for fabricating label-free electrochemical impedance genosensor. Graphene, with the structure of a single-atom-thick sheet of sp^2-bonded carbon atoms, was anchored to 1-aminopyrene (1-Ap) with the pyrenyl group *via* π-stacking interaction. The morphology, conductivity, and interaction of ApG hybrids were characterized by transmission electron microscopy (TEM), cyclic voltammetry (CV), electrochemical impedance spectroscopy (EIS), UV-visible (UV-vis) and fluorescence spectra. The amino-substituted oligonucleotide probe was conjugated to 1-Ap by the cross-linker glutaraldehyde. The DNA hybridization reaction of oligonucleotide probe with target DNA was monitored by EIS. Under optimum conditions, the proposed biosensor exhibited high sensitivity and a low detection limit for detecting the complementary oligonucleotide. The target oligonucleotide could be quantified in a wide range of 1.0×10^{-12} to 1.0×10^{-8} M with good linearity ($R = 0.9900$) and low detection limit of 4.5×10^{-13} M ($S/N = 3$).

1 Introduction

Graphene, with the structure of a single-atom-thick sheet of sp^2-bonded carbon atoms in a closely packed honeycomb two-dimensional lattice, was isolated by mechanically peeling off graphite crystals in 2004.[1–5] Due to its unique physical properties such as high specific surface area, rapid heterogeneous electron transfer,[6,7] great mechanical strength[8] and relatively low manufacturing cost,[9] graphene has drawn a lot of attention in recent years. Considering its biocompatibility,[10] graphene is an ideal material for the preparation of electrochemical biosensors.[11–18] Chen *et al.*[17] have reported a specific protein detection biosensor using thermally reduced graphene oxide sheets decorated with gold nanoparticle–antibody conjugates. Ju *et al.*[18] have proposed an electrochemical immunosensing method with graphene and gold nanoparticles using a triple signal amplification strategy for cancer biomarker detection.

However, graphene tends to form agglomerates through van der Waals interactions.[19,20] To prevent graphene from aggregating, hybrid structures are of particular importance which can be achieved by covalent or non-covalent attachment of other molecules onto graphene sheets.[21–23] Thereinto, non-covalent functionalization of graphene based on π-stacking interaction between graphene sheets and aromatic organic molecules does not disrupt the conjugation of the graphene sheets, and can improve its stability.[24] Müllen *et al.*[25] and Shi *et al.*[26] have reported that graphene could be stabilized in aqueous solution by large aromatic molecules based on a π-stacking interaction. 1-Aminopyrene (1-Ap), a bifunctional molecule with an amino functional group and a pyrenyl group, is highly aromatic in nature.[27] Because the pyrenyl group can interact strongly with the basal plane of graphene *via* π-stacking interaction, 1-Ap can irreversibly anchor to the large hydrophobic surface of graphene *via* simple ultrasonic treatment at room temperature. The preparation process doesn't need strong oxidants or corrosive acids and hence doesn't produce a large amount of hazardous waste, requiring no high cost after treatment. The mild, low-cost and eco-friendly non-covalent functionalization of graphene based on 1-Ap can avoid unwanted defects to graphene and preserve its integrity and the electronic structure.[28]

DNA quantitative assay has received great attention nowadays owning to its vital role in numerous inherited human disorders.[29] In addition, pathogens can be detected by quantitatively assaying their unique nucleic acid sequences.[30–35] Various techniques such as electrochemiluminescence,[36] electrochemistry,[37,38] fuorescence[39,40] and quartz crystal microbalance[41] have been developed for DNA detection. Among them, electrochemical genosensor possesses enormous promise due to its fast, simple and inexpensive characters in specific DNA target sequences analysis.[42–45]

Electrochemical impedance spectroscopy (EIS) has been proven to be a most powerful and sensitive tool for probing the features of surface-modified electrodes and widely applied to

[a]*College of Sciences, Shanghai University, Shanghai 200444, PR China. E-mail: luoliqw@yahoo.com.cn; Tel: +86 21 66134734*

[b]*Laboratory of Biosensing Technology, School of Life Sciences, Shanghai University, Shanghai 200444, PR China*

[c]*State Key Laboratory of Electroanalytical Chemistry, Changchun Institute of Applied Chemistry, Chinese Academy of Sciences, Changchun 130022, PR China. E-mail: wangzx@ciac.jl.cn; Tel: +86 431 85262243*

the detection of target DNA sequences.[46–49] Jiao *et al.*[50] have developed nanocomposite membrane for electrochemical impedance sensing of the immobilization and hybridization of DNA using nanosized shuttle-shaped cerium oxide, single-walled carbon nanotubes and ionic liquid 1-butyl-3-methylimidazolium hexafluorophosphate. Pumera and Bonanni[51] have constructed an efficient DNA impedance biosensing platform combining the sensitivity of EIS with the high selectivity of DNA hairpin probes for the rapid detection of single nucleotide polymorphism related to Alzheimer's disease. Niu *et al.*[22] have developed a novel *N*,*N*-bis-(1-aminopropyl-3-propylimidazol salt)-3,4,9,10-perylene tetracarboxylic acid diimide/graphene platform for label-free impedance sensing for conserved sequence of the pol gene of HIV-1.

Herein, a simple novel ApG hybrid-based label-free electrochemical impedance genosensor has been fabricated for detecting DNA with high sensitivity and selectivity. 1-Ap was chosen for preparing the graphene hybrids and fabricating electrochemical impedance genosensor since the pyrenyl group can interact strongly with the basal plane of graphene *via* π-stacking interaction,[52] and the amino groups of 1-Ap can be conjugated to amino-substituted oligonucleotide probes by the cross-linker glutaraldehyde (GA). In addition, the mild, low-cost and eco-friendly non-covalent functionalization of graphene based on π-stacking interaction between graphene sheets and 1-Ap molecules has the advantage of improving the stability of graphene and preserving its intrinsic properties, such as high specific surface area, good electrical conductivity and biocompatibility. The as-prepared electrochemical impedance genosensor also shows excellent reproducibility and provides potential applications in bioanalysis.

2 Experimental

2.1 Reagents

KH_2PO_4, $K_2HPO_4 \cdot 3H_2O$, NaCl, $K_3Fe(CN)_6$ and $K_4Fe(CN)_6 \cdot 3H_2O$ were provided by Sinopharm Chemical Reagent Beijing Co., Ltd. Graphite oxide (GO) was obtained from Nanjing XFNANO Materials Tech Co., Ltd, (Nanjing, China). Hydrazine hydrate ($NH_2NH_2 \cdot H_2O$, 80%) was purchased from Aladdin (Shanghai, China). 1-Ap was purchased from Tokyo Chemical Industry Co., Ltd, (Tokyo, Japan). GA (25%) was provided by Sigma (USA). Milli-Q water (18.25 MΩ cm) was used throughout the experiments.

24-base synthetic oligonucleotide specific sequences for colitoxin[53] were provided by Sangon Biotech Co., Ltd, (Shanghai, China):

• Probe ssDNA (PDNA): 5′-(NH_2-C_6)-GAG CGG CGC AAC ATT TCA GGT CGA-3′;

• Complementary ssDNA (CDNA): 5′-TCG ACC TGA AAT GTT GCG CCG CTC-3′;

• One mismatch-containing ssDNA (C_1DNA): 5′-TCG ACC TGA AAC GTT GCG CCG CTC-3′;

• Non-complementary ssDNA (NDNA): 5′-GAG CGG CGC AAC ATT TCA GGT CGA-3′.

The DNAs were dissolved in 50 mM Tris–HCl–0.1 M NaCl–0.2 M KCl–5 mM $MgCl_2$ (pH 7.4) buffer.

2.2 Instruments and characterizations

Transmission electron microscopy (TEM) images were obtained by a Hitachi H-600 (Japan, at an acceleration voltage of 100 kV). UV-vis absorption spectra were recorded using a UV-2501PC spectrometer (Shimadzu, Japan). Fluorescence emission spectra were recorded using a RF-5301PC spectrofluorometer with an excitation wavelength of 356.0 nm in a 1 cm quartz cell. Both excitation and emission slit widths were 1.5 nm. EIS measurements were tested by a Solartron 1255B Frequency Response Analyzer/SI 1287 Electrochemical Interface (Scribner Associates, Inc.) using 10 mM $[Fe(CN)_6]^{3-/4-}$ as the electrochemical probe. 5 mV amplitude of sine voltage signal was applied to the three-electrode system under open circuit potential, and the frequency varied from 0.1 Hz to 100 kHz. Cyclic voltammetry (CV) measurements were performed on a CHI 660D electrochemical workstation (Shanghai CH Instrument Co., China). A conventional three-electrode system was used with a saturated calomel electrode as the reference electrode, a platinum sheet as the counter electrode, and a modified glassy carbon electrode (GCE, 1 mm in diameter) as the working electrode. Prior to surface coating, the GCE was polished carefully with 1.0, 0.3 and 0.05 μm alumina powder, successively. Then, the polished GCE was cleaned sequentially with 1 : 1 HNO_3, ethanol and water with continuous sonicating for 3 min, respectively. Afterwards, the GCE was continuously scanned within a potential range of −1.0 V to +1.0 V in freshly prepared deoxygenated 0.5 M H_2SO_4 for 15 cycles to activate the GCE surface. The electrode was allowed to dry at ambient temperature for further use.

2.3 Preparation of graphene and ApG hybrids

Graphene was prepared according to the literature reports.[54–56] Briefly, 5 mg GO was dispersed in 50 mL water and the GO dispersion was exfoliated by sonicating under ambient conditions for 40 min generating claybank transparent solution. Then, $NH_2NH_2 \cdot H_2O$ (1% v/v) was added into the GO dispersion. The resulting mixture was heated to 100 °C and kept stirring for 24 h. Subsequently, the solution was filtered, and the filtration residue was dried in vacuum at 60 °C. Finally, black hydrophobic powder graphene was obtained and stored under ambient condition.

0.1 g graphene and 0.1 g 1-Ap were added into 20 mL ethanol, and the solution was treated with continuous sonicating for 1 h to form a lilac transparent solution and then stirring mechanically for 24 h at room temperature. The solution obtained was filtered using a nylon filter membrane and the filtration residue was rinsed with water for several times. Finally, the products (ApG hybrids) were dried in a vacuum oven at 80 °C for 3.5 h and then collected for further use.

2.4 Fabrication of electrochemical impedance genosensor

A schematic diagram of electrochemical impedance genosensor is displayed in Fig. 1. ApG was dissolved in 0.5% (w/w) GA solution to form homogeneous black ink-like GAApG solution (1 mg mL^{-1}) under ultrasonic vibration. 5 μL of the prepared solution was dropped onto the surface of GCE and kept for 1 h

at 35 °C in the oven to form GAApG/GCE. Then, the GAApG/GCE was rinsed with deionized water and dried under an N_2 stream. Subsequently, 10 μL of 2.5 μM PDNA was dropped on the surface of the GAApG/GCE and incubated for another 2 h at 35 °C to obtain PDNA/GAApG/GCE. Finally, the PDNA/GAApG/GCE was rinsed carefully with 0.1 M PBS containing 0.01 M NaCl (pH 7.4), dried under an N_2 stream and stored at 4 °C for further use.

2.5 Hybridization and electrochemical measurements of the genosensor

The hybridization procedure was performed by dropping 10 μL analyte solution (CDNA, C_1DNA or NDNA) with desired concentration onto the surface of PDNA/GAApG/GCE and reacting for 40 min at 35 °C, respectively. Then, the hybridized electrode was rinsed with 0.1 M PBS containing 0.01 M NaCl (pH 7.4) to remove the non-specifically adsorbed target DNAs. After hybridization reaction, the electrodes were named as CDNA-PDNA/GAApG/GCE, C_1DNA-PDNA/GAApG/GCE and NDNA-PDNA/GAApG/GCE, respectively.

3 Results and discussion

3.1 Characterizations of the graphene and ApG hybrids

Graphene has unique properties of high specific surface area, good electrical conductivity and biocompatibility. It is electronically a good low-noise material in molecular sensing, and very suitable for EIS determination of biorecognition events.[57–60] However, graphene tends to form agglomerates through van der Waals interactions. This agglomeration has two negative effects: first, it may reduce the surface area; and second, it may reduce access of electrolyte ions. To overcome this, a simple but robust strategy was presented to fabricate ApG hybrids. Because the pyrenyl group can interact strongly with the basal plane of graphene *via* π-stacking interaction, 1-Ap can strongly anchor to the large hydrophobic surface of graphene *via* simple ultrasonic treatment at room temperature.

The morphologies of the prepared graphene and ApG hybrids were characterized by TEM, as shown in Fig. 2. Fig. 2A reveals the typical wrinkled structure of graphene sheet, illustrating that graphene sheets are difficult to be dispersed in aqueous solution and always reunite to high-density large aggregates. To overcome this, 1-Ap was used to functionalize graphene in this work. Since the large hydrophobic surface of graphene can interact strongly with the pyrenyl group of 1-Ap, 1-Ap can anchor to the basal plane of graphene *via* π-stacking interaction.[27] In addition, the residual oxygen-containing functionalities on the basal plane of graphene could also absorb 1-Ap molecules through hydrogen bonding interaction,[28,52,61] causing aggregates (the back dots) on some places of the graphene surface, as shown in Fig. 2B.

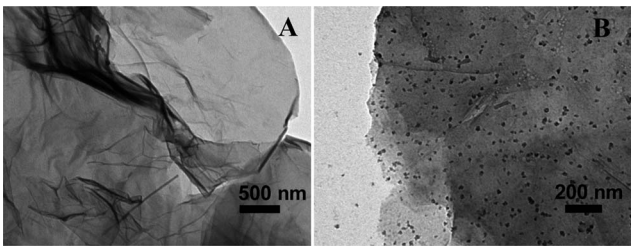

Fig. 2 TEM micrographs of graphene (A) and ApG hybrids (B).

The graphene and ApG hybrids were characterized by UV-vis and fluorescence spectra (as shown in Fig. 3). Fig. 3A illustrates the absorption spectra of GO, graphene, Ap and ApG hybrids in aqueous solution. The spectrum of the GO dispersion (curve a in the inset) exhibited a strong absorption band at 230 nm attributing to π–π* transitions of aromatic C·C bonds.[62] After GO was reduced to graphene (curve b in the inset), the absorption band red-shifted to 275 nm, indicating the restoration of π-conjugation network. The spectrum of 1-Ap (curve c) appeared three characteristic adsorption peaks, which were located in the near-ultraviolet region around 241.0, 280.5 and 355.0 nm, respectively. The three corresponding absorption peaks were also observed at the spectrum of ApG (curve d), indicating the presence of 1-Ap molecules on graphene sheet. The broadening of three relevant peaks in the spectrum of ApG provides further evidence on the interaction between graphene and 1-Ap. This phenomenon is the same as that of 1-Ap on the sidewalls of MWCNTs[27,63] and thionine on graphene sheet.[56]

Fluorescence spectra were performed to study the π-stacking interaction between 1-Ap and graphene. Fig. 3B shows the fluorescence spectra of graphene (inset), 1-Ap (curve c) and ApG hybrids (curve d), respectively. 1-Ap aqueous solution exhibited a broad fluorescence band around at 438.0 nm. When 1-Ap was stacked on the surface of graphene by π–π interaction, its fluorescence was significantly quenched. The high efficiency quenching was considered as the direct consequence of non-covalent binding of 1-Ap on the graphene surface which acted as a "nanoquencher" of the pyrene rings due to fluorescence resonance energy transfer (FRET).[40,64] The planar configuration of graphene and pyrene rings guarantees the close proximity of 1-Ap with graphene, thus giving rise to the efficient fluorescence quenching due to π-stacking interaction between graphene and pyrene rings. The results confirmed the successful noncovalent binding between 1-Ap and graphene.

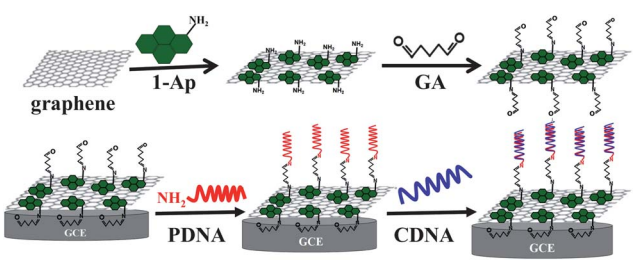

Fig. 1 Schematic diagram of the electrochemical impedance genosensor.

3.2 Electrochemical characterization of different electrodes

Fig. 4 shows the CVs and the Nyquist diagrams of 10 mM $[Fe(CN)_6]^{3-/4-}$ (1 : 1) at different electrodes. As shown in Fig. 4A, the peak current of $[Fe(CN)_6]^{3-/4-}$ at GAApG/GCE (curve b) was lower than that of the bare electrode (curve a) and potential difference between the oxidation and reduction peaks became

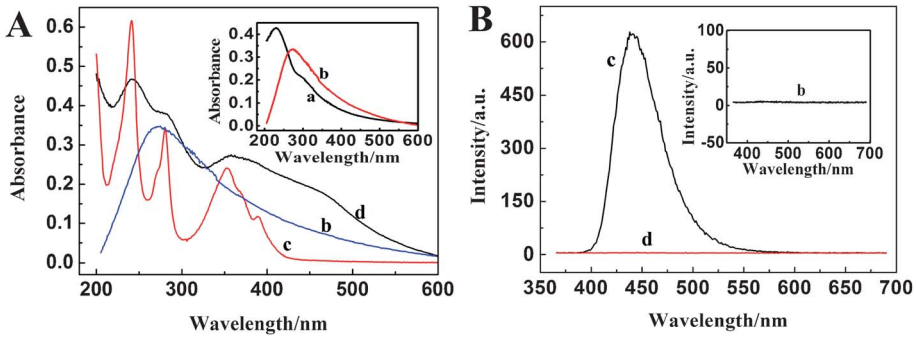

Fig. 3 (A) UV-vis spectra of GO (a), graphene (b), 1-Ap (c) and ApG hybrids (d) in aqueous solution; (B) Corresponding fluorescence spectra of graphene (b), 1-Ap (c) and ApG hybrids (d) in aqueous solution, excitation wavelength: 356.0 nm.

larger, suggesting that redox reversibility of $[Fe(CN)_6]^{3-/4-}$ became poorer. The peak current of $[Fe(CN)_6]^{3-/4-}$ at PDNA/GAApG/GCE (curve c) was smaller than that of GAApG/GCE (curve b), indicating that the PDNA was successfully fixed on the surface of the GAApG/GCE. This was due to the negative charge of phosphoric acid groups on the single stranded probe DNA interfered the diffusion of electronegative $[Fe(CN)_6]^{3-/4-}$ to the electrode surface.[65–67] When probe DNA and target complementary DNA hybridized, the peak current of $[Fe(CN)_6]^{3-/4-}$ at CDNA/PDNA/GAApG/GCE (curve d) decreased further (curve c).

EIS has been proved as a very powerful tool for investigating the interfacial properties (*i.e.* resistance and capacitance) of conductive or semi-conductive surfaces. It is also a label-free technique for sensitively studying biorecognition events at the electrode surface. Fig. 4B shows the Nyquist diagrams of different modified electrodes, where R_{et} stands for interfacial electron transfer resistance in the equivalent circuit. Compared to that of the bare electrode, R_{et} of GAApG/GCE increases from 68.1 Ω (curve a) to 465.3 Ω (curve b), revealing that GAApG has been successfully fixed on the surface of GCE. The macrocyclic 1-Ap and the long carbon chain GA block the electron transfer of the redox probe $[Fe(CN)_6]^{3-/4-}$ to the electrode surface, resulting in the increase of R_{et} of GAApG/GCE. After covalently immobilized PDNA on the electrode surface, R_{et} of PDNA/GAApG/GCE continually increased, which reachs 727.3 Ω (curve c). When PDNA/GAApG/GCE has been hybridized with 10^{-9} M CDNA, the R_{et} of CDNA/PDNA/GAApG/GCE is further increased to 1059.6 Ω (curve d). This continually increased R_{et} is due to that the negatively charged DNA strands hindered the $[Fe(CN)_6]^{3-/4-}$ diffusing to electrode surface, which was consistent with the results of CVs.

3.3 Optimization of the sensing conditions

As shown in Fig. 5A, the effect of hybridization time on EIS signals of CDNA/PDNA/GAApG/GCE has been investigated in 0.1 M PBS (pH 7.4) containing 0.01 M NaCl and 10 mM $Fe(CN)_6^{3-/4-}$ (1 : 1). In this case, the DNA biosensor was incubated in 1.0 nM

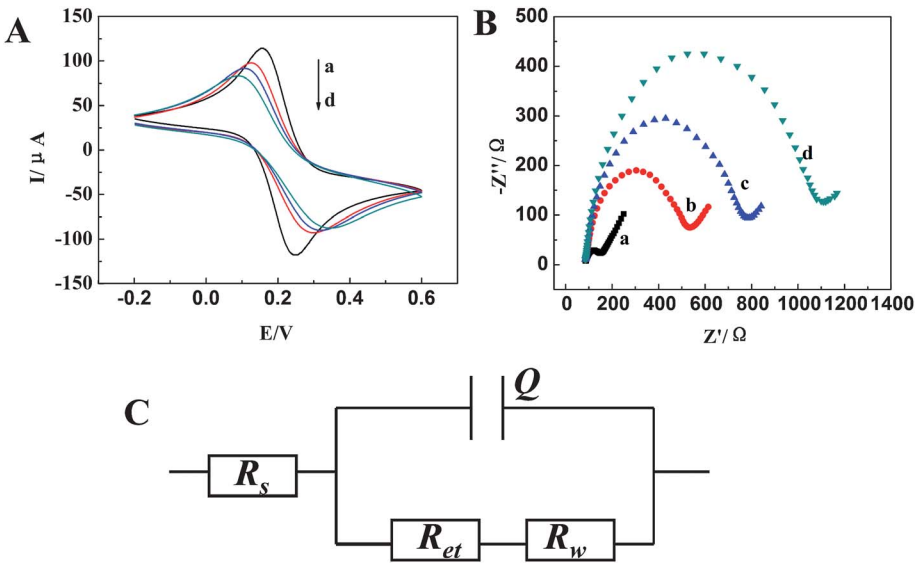

Fig. 4 CVs (A) and Nyquist diagrams (B) of GCE (a), GAApG/GCE (b), PDNA/GAApG/GCE (c) and 1 nM CDNA/PDNA/GAApG/GCE (d) in 0.1 M PBS (pH 7.4) contained 0.01 M NaCl and 10 mM $Fe(CN)_6^{3-/4-}$ (1 : 1). Equivalent circuit voltammograms (C): R_s, Q, R_{et} and R_w represent the resistance of the electrolyte solution, the value of constant phase element, the charge-transfer resistance and the Warburg impedance, respectively. The frequency varied from 0.1 to 100 kHz, and 5 mV amplitude of the sine voltage signal was used.

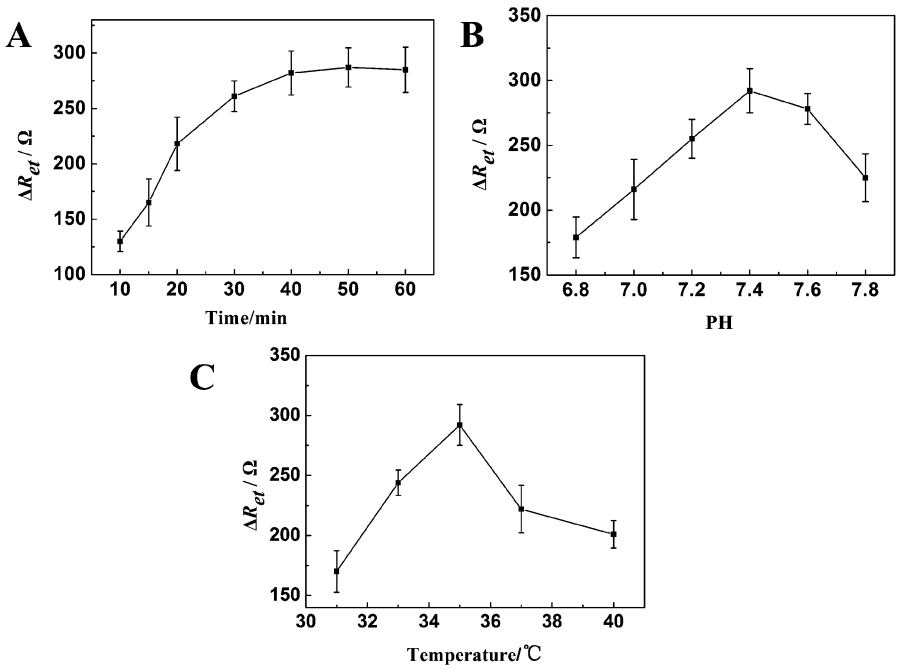

Fig. 5 Effects of hybridization time (A), hybridization pH (B) and hybridization temperature (C) on ΔR_{et}. The frequency varied from 0.1 Hz to 100 kHz, and 5 mV amplitude of the sine voltage signal was used.

CDNA at 35 °C for varying time periods from 10 to 60 min. The signal difference between R_{et} value (ΔR_{et}) of the PDNA/GAApG/GCE and that of CDNA/PDNA/GAApG/GCE was adopted as the measurement signal in the experiment, *i.e.*, $\Delta R_{et} = R_{et,CDNA} - R_{et,PDNA}$. As shown in Fig. 5A, ΔR_{et} is rapidly increased with increasing the hybridization time from 10 to 40 min, and then become saturated after 40 min. Considering the sensitivity and assay time, 40 min is adopted as optimized hybridization time.

Because the highest R_{et} value is obtained at solution pH value of 7.4, the electrochemical detection is performed at pH 7.4 in our study (as shown in Fig. 5B). In addition, the ΔR_{et} is also affected by the hybridization temperature, peak value of ΔR_{et} is obtained at 35 °C. Therefore, 35 °C is selected as optimized hybridization temperature in our further experiment.

3.4 Label-free oligonucleotides detection with the proposed impedance genosensors

Under optimized experimental conditions (the PDNA/GAApG/GCE is reacted with CDNA at 35 °C for 40 min), ΔR_{et} was found to increase linearly with the increasing the concentration of CDNA in the reaction solution from 1.0×10^{-12} M to 1.0×10^{-8} M with regression equation $\Delta R_{et}\,(\Omega) = 81.8\lg C\,(\mathrm{M}) + 1070.0$ and correlation coefficient of 0.9900. The detection limit was estimated to be 4.5×10^{-13} M with 3σ (where σ was the relative standard deviation of 11 parallel measurements of the blank solution). Table 1 lists the sensor performance compared with other modified electrodes for the determination of targeted DNA.[68–71] As can be seen from Table 1, our proposed electrochemical impedance genosensor shows excellent sensitivity and wide dynamic range (Fig. 6).

3.5 The selectivity and reproducibility of the electrochemical impedance genosensor

It is important to develop cost-effective methods for identifying point mutations in DNA sequences because of the application of the single nucleotide polymorphisms (SNPs) in medical diagnosis. Using our electrochemical impedance genosensor, we have investigated a simple case in which one perfect match

Table 1 Comparison of the performance of different sensors

Method	Modifier	Redox probe	Linear range (M)	Detection limit (M)	Ref.
SWV	Poly$[G]_{20}$-biobarcode nanoparticles	$Ru(bpy)_3^{2+}$	10^{-12} to 10^{-8}	1.0×10^{-12}	33
EIS	CeO_2–SWNTs–$BMIMPF_6$	$[Fe(CN)_6]^{3-/4-}$	10^{-12} to 10^{-7}	2.3×10^{-13}	50
EIS	NH_2–G_4PAMAM dendrimers	$[Fe(CN)_6]^{3-/4-}$	10^{-11} to 10^{-8}	3.8×10^{-12}	65
EIS	nano-SiO_2–PATP film	$[Fe(CN)_6]^{3-/4-}$	10^{-11} to 0^{-6}	1.5×10^{-12}	66
EIS	Chitosan–MWNTs	$[Fe(CN)_6]^{3-/4-}$	10^{-13} to 5×10^{-10}	8.5×10^{-14}	67
EIS	APTES–graphene	$[Fe(CN)_6]^{3-/4-}$	10^{-12} to 10^{-6}	10^{-13}	68
DPV	Prussian Blue–chitosan	Daunomycin	2.12×10^{-11} to 2.12×10^{-8}	1.58×10^{-11}	69
EIS	ER–GO	$[Fe(CN)_6]^{3-/4-}$	10^{-11} to 10^{-6}	2.5×10^{-12}	70
EIS	PTCA–graphene	$[Fe(CN)_6]^{3-/4-}$	1.0×10^{-12} to 1.0×10^{-6}	5.0×10^{-13}	71
EIS	ApG–graphene	$[Fe(CN)_6]^{3-/4-}$	10^{-12} to 10^{-8}	4.5×10^{-13}	This work

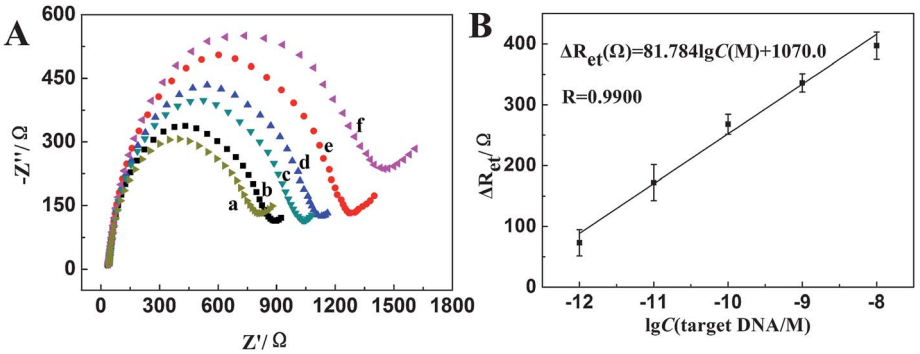

Fig. 6 (A) Nyquist diagrams recorded at PDNA/GAApG/GCE (a) and after hybridization with different concentrations of CDNA: 1.0×10^{-12} M (b), 1.0×10^{-11} M (c), 1.0×10^{-10} M (d), 1.0×10^{-9} M (e), and 1.0×10^{-8} M (f) in 0.1 M PBS (pH 7.4) contained 0.01 M NaCl and 10 mM $Fe(CN)_6^{3-/4-}$ (1 : 1). (B) Corresponding data analysis of (A). The frequency varied from 0.1 Hz to 100 kHz, and 5 mV amplitude of sine voltage signal was used.

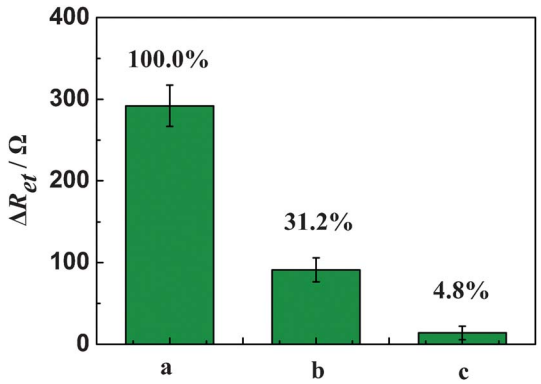

Fig. 7 ΔR_{et} of CDNA/PDNA/GAApG/GCE (a), C_1DNA/PDNA/GAApG/GCE (b), and NDNA/PDNA/GAApG/GCE (c) in 0.1 M PBS (pH 7.4) contained 0.01 M NaCl and 10 mM $Fe(CN)_6^{3-/4-}$ (1 : 1), respectively. The concentration of DNA is 1 nM in hybridization solution. The frequency varied from 0.1 Hz to 100 kHz, and 5 mV amplitude of the sine voltage signal was used.

oligonucleotide (CDNA), one oligonucleotide with a single base mutation (C_1DNA) and one non-complementary oligonucleotide (NDNA) were hybridized with PDNA. As shown in Fig. 7, hybridization is only effective with the oligonucleotide sequence strictly complementary to the PDNA; for instance, ΔR_{et} values of C_1DNA/PDNA/GAApG/GCE and NDNA/PDNA/GAApG/GCE are 31.2 and 4.8% of CDNA/PDNA/GAApG/GCE, respectively. The experimental results indicate that the electrochemical impedance genosensor has reasonable selectivity and can be used to detect SNP.

To characterize reproducibility of this label-free impedance electrochemistry genosensor, three trials were run, using PDNA/GAApG/GCEs from several batches prepared on different days. The PDNA/GAApG/GCEs were hybridized with 1 nM CDNA under the optimized experimental conditions, respectively. An acceptable relative standard deviation (RSD) of 9.5% ($n = 3$) for ΔR_{et} value was estimated, showing that the impedance electrochemistry genosensor has high reproducibility.

4 Conclusions

This work presents a simple and effective label-free electrochemical impedance genosensor based on ApG hybrids for sensitive determination of DNA with high selectivity by monitoring ΔR_{et} caused by the DNA hybridization reaction. Non-covalent functionalization of graphene by 1-Ap based on π-stacking interaction could improve the stability of graphene and preserve its intrinsic properties of high specific surface area, good electrical conductivity and biocompatibility. As proof-of-principle experiments, the detection and SNP analysis of 24-mer oligonucleotide (based on the coli toxin sequence) have been carefully studied. The experimental results suggest that our approach could be used as a low cost technique for genetic studies including SNP analysis and low abundance transcripts in cells.

Acknowledgements

The authors would like to thank the National Science Foundation of China (no. 21271127, 61171033) and the Leading Academic Discipline Project of Shanghai Municipal Education Commission (J50102) for financial supports.

References

1 K. S. Novoselov, A. K. Geim, S. V. Morozov, D. Jiang, Y. Zhang, S. V. Dubonos, I. V. Grigorieva and A. A. Firsov, *Science*, 2004, **306**, 666–669.
2 J. C. Meyer, A. K. Geim, M. I. Katsnelson, K. S. Novoselov, T. J. Booth and S. Roth, *Nature*, 2007, **446**, 60–63.
3 C. H. Lu, H. H. Yang, C. L. Zhu, X. Chen and G. N. Chen, *Angew. Chem., Int. Ed.*, 2009, **48**, 4785–4787.
4 C. N. Rao, A. K. Sood, K. S. Subrahmanyam and A. Govindaraj, *Angew. Chem., Int. Ed.*, 2009, **48**, 7752–7777.
5 B. G. Choi, H. Park, M. H. Yang, Y. M. Jung, S. Y. Lee, W. H. Hong and T. J. Park, *Nanoscale*, 2010, **2**, 2692–2697.
6 M. Pumera, *Chem. Soc. Rev.*, 2010, **39**, 4146–4157.
7 L. A. L. Tang, J. Wang and K. P. Loh, *J. Am. Chem. Soc.*, 2010, **132**, 10976–10977.
8 X. Zhao, Q. H. Zhang and D. J. Chen, *Macromolecules*, 2010, **43**, 2357–2363.
9 M. Segal, *Nat. Nanotechnol.*, 2009, **4**, 612–614.
10 H. Chen, M. B. Muller, K. J. Gilmore, G. G. Wallace and D. Li, *Adv. Mater.*, 2008, **20**, 3557–3561.

11 Y. Du, S. J. Guo, S. J. Dong and E. K. Wang, *Biomaterials*, 2011, **32**, 8584–8592.
12 C. Shan, H. Yang, J. Song, D. Han, A. Ivaska and L. Niu, *Anal. Chem.*, 2009, **81**, 2378–2382.
13 Y. Wang, Y. M. Li, L. H. Tang, J. Lu and J. H. Li, *Electrochem. Commun.*, 2009, **11**, 889–892.
14 X. H. Kang, J. Wang, H. Wu, I. A. Aksay, J. Liu and Y. H. Lin, *Biosens. Bioelectron.*, 2009, **25**, 901–905.
15 L. Y. Feng, Y. Chen, J. S. Ren and X. G. Qu, *Biomaterials*, 2011, **32**, 2930–2937.
16 L. J. Bai, R. Yuan, Y. Q. Chai, Y. Zhuo, Y. L. Yuan and Y. Wang, *Biomaterials*, 2012, **33**, 1090–1096.
17 S. Mao, G. H. Lu, K. H. Yu, Z. Bo and J. H. Chen, *Adv. Mater.*, 2010, **22**, 3521–3526.
18 D. J. Lin, J. Wu, M. Wang, F. Yan and H. X. Ju, *Anal. Chem.*, 2012, **84**, 3662–3668.
19 D. Li, M. B. Müller, S. Gilje, R. B. Kaner and G. G. Wallace, *Nat. Nanotechnol.*, 2008, **3**, 101–105.
20 Y. Y. Cai, H. Li, B. Du, M. H. Yang, Y. Li, D. Wu, Y. F. Zhao, Y. X. Dai and Q. Wei, *Biomaterials*, 2011, **32**, 2117–2123.
21 Z. Zhang, J. Zhang, B. L. Zhang and J. L. Tang, *Nanoscale*, 2013, **5**, 118–123.
22 Y. W. Hu, K. K. Wang, Q. X. Zhang, F. H. Li, T. S. Wu and L. Niu, *Biomaterials*, 2012, **33**, 1097–1106.
23 Z. Z. Lv, X. Yang and E. K. Wang, *Nanoscale*, 2013, **5**, 663–670.
24 A. Ghosh, K. V. Rao, S. J. George and C. N. R. Rao, *Chem.–Eur. J.*, 2010, **16**, 2700–2704.
25 Q. Su, S. P. Pang, V. Alijani, C. Li, X. L. Feng and K. Müllen, *Adv. Mater.*, 2009, **21**, 3191–3195.
26 Y. X. Xu, H. Bai, G. W. Lu, C. Li and G. Q. Shi, *J. Am. Chem. Soc.*, 2008, **130**, 5856–5857.
27 S. Y. Wang, X. Wang and S. P. Jiang, *Langmuir*, 2008, **24**, 10505–10512.
28 J. Liu, J. Tang and J. J. Gooding, *J. Mater. Chem.*, 2012, **22**, 12435–12452.
29 J. C. Chamcheu, I. A. Siddiqui, D. N. Syed, V. M. Adhami, M. Liovic and H. Mukhtar, *Arch. Biochem. Biophys.*, 2011, **508**, 123–137.
30 J. H. Jung, D. S. Cheon, F. Liu, K. B. Lee and T. S. Seo, *Angew. Chem., Int. Ed.*, 2010, **49**, 5708–5711.
31 Z. F. Liu, L. H. Jiang, F. Gali, I. Nederlof, R. C. L. Olsthoorn, G. E. M. Lamers, T. H. Oosterkamp and J. P. Abrahams, *Adv. Funct. Mater.*, 2010, **20**, 2857–2865.
32 Q. B. Wang, J. P. Lei, S. Y. Deng, L. Zhang and H. X. Ju, *Chem. Commun.*, 2013, **49**, 916–918.
33 Q. Wang, J. Su, J. Xu, Y. Xiang, R. Yuan and Y. Q. Chai, *Sens. Actuators, B*, 2012, **163**, 267–271.
34 F. Lucarelli, G. Marrazza, A. P. Turner and M. Mascini, *Biosens. Bioelectron.*, 2004, **19**, 515–530.
35 M. Minunni, S. Tombelli, J. Fonti, M. M. Spiriti, M. Mascini, P. Bogani and M. Buiatti, *J. Am. Chem. Soc.*, 2005, **127**, 7966–7967.
36 D. Zhu, Y. Tang, D. Xing and W. R. Chen, *Anal. Chem.*, 2008, **80**, 3566–3571.
37 R. Miranda-Castro, P. de-Los-Santos-Alvarez, M. J. Lobo-Castañón, A. J. Miranda-Ordieres and P. Tuñón-Blanco, *Anal. Chem.*, 2007, **79**, 4050–4055.
38 A. Erdem, M. I. Pividori, A. Lermo, A. Bonanni, M. D. Valle and S. Alegret, *Sens. Actuators, B*, 2006, **114**, 591–598.
39 R. Yang, J. Jin, Y. Chen, N. Shao, H. Kang, Z. Xiao, Z. Tang, Y. Wu, Z. Zhu and W. Tan, *J. Am. Chem. Soc.*, 2008, **130**, 8351–8358.
40 F. Liu, J. Y. Choi and T. S. Seo, *Biosens. Bioelectron.*, 2010, **25**, 2361–2365.
41 Y. H. Fei, X. Y. Jin, Z. S. Wu, S. B. Zhang, G. L. Shen and R. Q. Yu, *Anal. Chim. Acta*, 2011, **691**, 95–102.
42 J. P. Tosar, G. Brañas and J. Laíz, *Biosens. Bioelectron.*, 2010, **26**, 1205–1217.
43 M. Pumera, S. Sánchez, I. Ichinose and J. Tang, *Sens. Actuators, B*, 2007, **123**, 1195–1205.
44 S. Riccardi Cdos, H. Yamanaka, M. Josowicz, J. Kowalik, B. Mizaikoff and C. Kranz, *Anal. Chem.*, 2006, **78**, 1139–1145.
45 C. Jiang, T. Yang, K. Jiao and H. W. Gao, *Electrochim. Acta*, 2008, **53**, 2917–2924.
46 A. Kowalczyk, A. Nowicka, R. Jurczakowski, M. Fau, A. Krolikowska and Z. Stojek, *Biosens. Bioelectron.*, 2011, **26**, 2506–2512.
47 X. G. Liu, X. J. Qu, J. Dong, S. Y. Ai and R. X. Han, *Biosens. Bioelectron.*, 2011, **26**, 3679–3682.
48 X. B. Zhu, S. Y. Ai, Q. P. Chen, H. S. Yin and J. Xu, *Electrochem. Commun.*, 2009, **11**, 1543–1546.
49 R. G. Cao, B. Zhu, J. J. Li and D. S. Xu, *Electrochem. Commun.*, 2009, **11**, 1815–1818.
50 W. Zhang, T. Yang, X. M. Zhuang, Z. Y. Guo and K. Jiao, *Biosens. Bioelectron.*, 2009, **24**, 2417–2422.
51 A. Bonanni and M. Pumera, *ACS Nano*, 2011, **5**, 2356–2361.
52 S. Kubota, T. Maruyama, H. Nishikiori, F. Ito, N. Tanaka, M. Endoc and T. Fujii, *J. Photochem. Photobiol., A*, 2011, **218**, 226–230.
53 H. Cai, N. N. Zhu, Y. Jiang, P. G. He and Y. Z. Fang, *Biosens. Bioelectron.*, 2003, **18**, 1311–1319.
54 S. W. Hummers and R. E. Offeman, *J. Am. Chem. Soc.*, 1958, **80**, 1339.
55 N. I. Kovtyukhova, P. J. Ollivier, B. R. Martin, T. E. Mallouk, S. A. Chizhik, E. V. Buzaneva and A. D. Gorchinskiy, *Chem. Mater.*, 1999, **11**, 771–778.
56 L. M. Zhu, L. Q. Luo and Z. X. Wang, *Biosens. Bioelectron.*, 2012, **35**, 507–511.
57 J. X. Wang, *Phys. Rev. B: Condens. Matter Mater. Phys.*, 2008, **78**, 245304.
58 Y. Wan, Z. F. Lin, D. Zhang, Y. Wang and B. R. Hou, *Biosens. Bioelectron.*, 2011, **26**, 1959–1964.
59 D. D. Zhang, Y. M. Zhang, L. Zheng, Y. Z. Zhan and L. C. He, *Biosens. Bioelectron.*, 2013, **42**, 112–118.
60 A. Bonanni, A. H. Loo and M. Pumera, *TrAC, Trends Anal. Chem.*, 2012, **37**, 12–21.
61 H. Matsumoto, Y. Koyama and A. Tanioka, *Langmuir*, 2002, **18**, 3698–3703.
62 X. M. Sun, Z. Liu, K. Welsher, J. T. Robinson, A. Goodwin, S. Zaric and H. Dai, *Nano Res.*, 2008, **1**, 203–212.
63 I. P. Chen, *Chem. Commun.*, 2013, **49**, 2753–2755.
64 H. X. Chang, L. H. Tang, Y. Wang, J. H. Jiang and J. H. Li, *Anal. Chem.*, 2010, **82**, 2341–2346.

65 A. X. Li, F. Yang, Y. Ma and X. R. Yang, *Biosens. Bioelectron.*, 2007, **22**, 1716–1722.
66 Y. Ma, K. Jiao, T. Yang and D. X. Sun, *Sens. Actuators, B*, 2008, **131**, 565–571.
67 Q. X. Wang, B. Zhang, X. Q. Lin and W. Weng, *Sens. Actuators, B*, 2011, **156**, 599–605.
68 Z. J. Wang, J. Zhang, P. Chen, X. Z. Zhou, Y. L.Yang, S. X. Wu, L. Niu, Y. Hand, L. H. Wang, P. Chen, F. Boey, Q. C. Zhang, B. Liedberg and H. Zhang, *Biosens. Bioelectron.*, 2011, **26**, 3881–3886.
69 Y. Bo, W. Q. Wang, J. F. Qi and S. S. Huang, *Analyst*, 2011, **136**, 1946–1951.
70 A. Bonanni, A. Ambrosi and M. Pumera, *Chem.–Eur. J.*, 2012, **18**, 1668–1673.
71 Y. W. Hu, F. H. Li, X. X. Bai, D. Li, S. C. Hua, K. K. Wang and L. Niu, *Chem. Commun.*, 2011, **47**, 1743–1745.